Analytical solution for a deep tunnel excavated in a porous elasto-plastic material considering the effects of seepage forces

R. E. Barbosa
EngSolutions, Inc., Ft. Lauderdale, Florida, USA

ABSTRACT: Seepage forces generated during tunnel excavation affect the ground response and may cause severe instability problems, including total ground collapse and flooding into the tunnel. This paper presents a new closed-form analytical solution, for stresses and displacements around a cylindrical tunnel excavated in a porous water-bearing elasto-plastic material, which includes the effects of seepage forces. The analysis is carried out in terms of effective stresses and pore water pressures. The solution shows that seepage forces may have a major effect on the effective stresses around the tunnel, on the extent of the plastic zone, on the radial displacements, and on the tunnel support requirements. The conditions for development of a 'flowing ground' condition at the tunnel face have been identified. The paper presents a procedure for the hydromechanical ground-support interaction analysis, to determine the excavation induced inflow and the pressures acting on the lining, throughout the progressive driving of the tunnel, including the effective pressures exerted by the ground and the pressures generated by the water.

1 INTRODUCTION

Tunneling in water bearing ground affects the hydraulic equilibrium of the surrounding ground leading to seepage into the tunnel. The seepage forces generated in the ground by the movement of water towards the tunnel can have a significant effect on the behavior of the opening. Groundwater inflow can cause severe instability problems, including total ground collapse and flooding into the tunnel. Numerous case histories of tunnel failures during construction, at sections with high water pressures, have been reported (e.g. Marulanda, et al, 2008, Singh et al, 2006). Failure often consists of a sudden "mud inrush" flowing violently into the opening, dragging equipment, facilities and sometimes even workers, and completely invading long stretches of tunnel. Even in less striking cases, seepage forces can have a strong effect on the ground support requirements and on the structural requirements of the support system.

Nevertheless, no adequate analytical solutions that consider the effect of seepage forces are currently available for analyzing the inelastic ground-support interaction to dimension tunnel support elements, and for properly assessing cases of 'flowing ground'.

A number of researchers have investigated the effect of seepage forces during excavation on the stress and displacement fields around tunnels. The analysis techniques used by these authors vary from advanced numerical methods to simplified elastic solutions. Alvarez (1997) used the coupled hydro-mechanical discrete-finite-element model developed by Barbosa (1990), Shin et al (2005) used a coupled finite element model with nonlinear permeability, Fernandez and Moon (2006) used a coupled distinct element model, Lee and Nam (2001, 2004) used uncoupled finite element analyses, and Li (1999) and Bobet (2003) developed elastic closed-form solutions.

In this paper a proper elasto-plastic solution is derived, for a deep cylindrical tunnel excavated in a Mohr-Coulomb perfectly plastic material under the water table, considering seepage

forces. In addition to establishing the radius of the plastic zone, radial convergence, the stress and displacement fields around the tunnel, and identifying the condition for development of flowing ground condition at the tunnel face, a procedure for hydromechanic ground-support interaction is proposed. The basic assumptions are stated first and then the solution is developed.

2 BASIC ASSUMPTIONS

The basic configuration considered in this study is shown in Figure 1. The analysis assumes a deep cylindrical tunnel of radius *a,* excavated in a naturally stressed water-bearing ground that obeys the principle of effective stress. A supporting lining is installed after excavation. A cylindrical coordinate system with the origin at the center of the opening is used in the analysis. The length of the tunnel is such that the problem can be treated two-dimensionally.

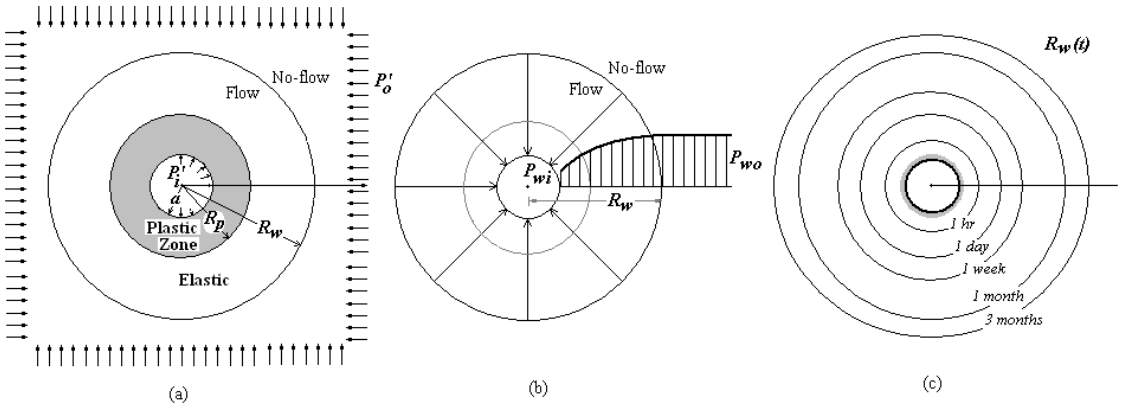

Figure 1. (a) Effective stresses (b) Pore water pressures (c) Transient hydraulic radius of influence.

The horizontal and vertical in situ effective stresses are assumed to be equal and to have a magnitude P'_0. The installed support is assumed to exert a uniform radial effective support pressure P'_i on the walls of the tunnel.

The original groundwater pressure is P_{w0}. The pressure inside the supported tunnel is equal to the atmospheric pressure. The water pressure at the lining-tunnel wall interface is P_{wi}. Groundwater inflow is assumed to be radial. It is assumed that the effect of the water-pressure-drop vanishes beyond a no-flow moving boundary located at a time-dependent distance $R_w(t)$.Beyond such instantaneous distance, the tunnel has no effect on the original groundwater condition and the pore water pressure becomes equal to the original ground water pressure.

The original ground is assumed to be a porous liner-elastic material characterized by a Young's modulus *E,* a Poisson's ratio *v*, a Darcy's coefficient of permeability *K,* and a specific storage S_s. The failure characteristics of this material are defined by the Coulomb-Navier equation.

$$\sigma_1^{'} = \sigma_c + \sigma_3^{'}.N_\phi \qquad N_\phi = \frac{1+\sin\phi^{'}}{1-\sin\phi^{'}} \tag{1}$$

where σ_c = unconfined compressive strength and ϕ' = effective friction angle.

The failed ground surrounding the tunnel is assumed to be perfectly plastic and to satisfy the following failure criterion

$$\sigma_1^{'} = \sigma_{cr} + \sigma_3^{'}.N_{\phi r} \qquad N_{\phi_r} = \frac{1+\sin\phi_r^{'}}{1-\sin\phi_r^{'}} \tag{2}$$

It is assumed that the strength reduces suddenly from the peak defined in equation (1) to the 'residual' defined in equation (2).

The volumetric response of the material in the plastic zone is controlled by the dilation angle α'. If the dilation angle is equal to the friction angle (α'=ϕ_r') then the plastic flow rule is said to be *associated* and the material undergoes volumetric expansion while it plastifies. If the dilation angle is less than the friction angle the plastic flow rule is said to be *non-associated*. If the dilation angle is zero, there is no volumetric change while the material plastifies. The dilation angle enters the solution through the parameter N_α that controls the ratio between the circumferential (or tangential) and the radial components of the plastic strain increment.

$$\frac{\Delta\varepsilon_\theta^{plastic}}{\Delta\varepsilon_r^{plastic}} = -\frac{1}{N_\alpha} \qquad N_\alpha = \frac{1+\sin\alpha'}{1-\sin\alpha'} \tag{3}$$

3 FUNDAMENTAL RELATIONS

3.1 *Equilibrium and compatibility*

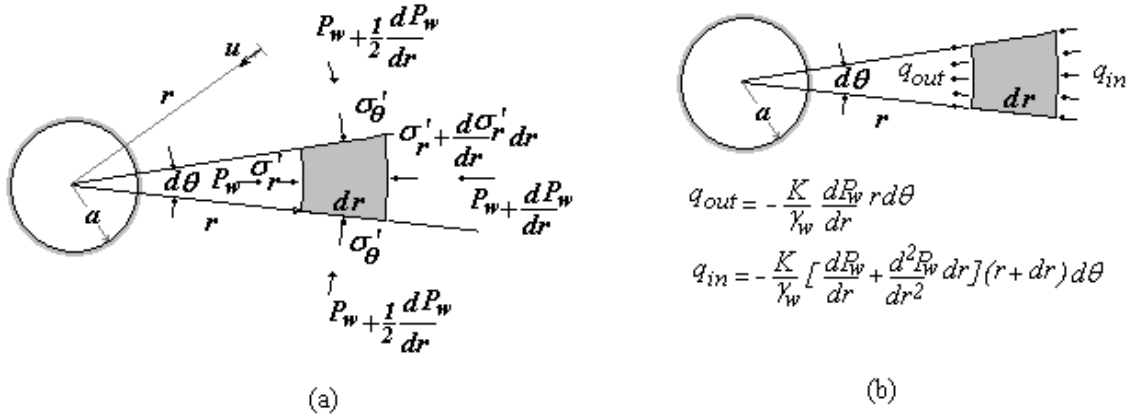

Figure 2. (a) Equilibrium of an infinitesimal element (b) Water continuity on infinitesimal element.

Figure 2(a) illustrates the stresses acting on a typical ground element. The basic differential equation of equilibrium for such element is

$$\frac{\partial\sigma'_r}{\partial r}+\frac{\sigma'_r-\sigma'_\theta}{r}+\frac{\partial P_w}{\partial r}=0 \tag{4}$$

where σ'_r and σ'_θ represent the effective radial and tangential stresses respectively at a distance *r*, and the third term is the seepage force. The radial and tangential strains for plane strain conditions can be stated in terms of the radial displacement *u,* as follows

$$\varepsilon_r=\frac{\partial u}{\partial r} \qquad \varepsilon_\theta=\frac{u}{r} \tag{5}$$

Strain components are related by the strain compatibility equation, which is obtained by eliminating the radial displacement in Eq. (5)

$$\frac{\partial\varepsilon_\theta}{\partial r}-\frac{\varepsilon_r-\varepsilon_\theta}{r}=0 \tag{6}$$

3.2 *Continuity*

Figure 2(b) illustrates the amount of water that enters a differential element and the amount of water that leaves the element, per unit time. The difference between these two quantities represents the change in the volume of water stored in the element. For a steady state condition, the amount of water that leaves the element is equal to the amount of water that enters it. In the transient stage, the flow rate that exits the element is larger than the flow rate that enters, as some water stored in voids and joints of the ground is released.

Using Darcy's law to write the flow rates in and out of the element and writing the change in volume of water in terms of the volumetric specific storage of the ground S_s, the continuity condition yields the following diffusion equation

$$\frac{\partial^2 P_w}{\partial r^2} + \frac{1}{r}\frac{\partial P_w}{\partial r} = \frac{S_s}{K}\frac{\partial P_w}{\partial t^2} \tag{7}$$

The volumetric specific storage is the amount of water per unit volume of a saturated formation that is released, per unit decline in hydraulic head. Specific storage can be expressed in terms of compressibility of water C_w, compressibility of skeleton C_s, and porosity n, as $S_s = \gamma_w(C_s + nC_w)$.

4 METHOD OF ANALYSIS

The method of analysis follows the approach used by Perrochet (2004) to derive a transient solution for tunnel discharge under constant drawdown. The analysis is based on the idea that the transient solution can be computed as successive steady state snapshots using a time dependent radius of influence, R_w. Therefore, in deriving the solution for stresses and displacements, the equilibrium equation is integrated, by treating the radius of influence as a known constant distance beyond which the water pressures becomes equal to the original water pressure P_{w0}. The transient nature of the solution is represented by the time dependency of R_w, which is determined from the solution of the diffusion equation.

The proposed solution includes coupling between effective stresses and pore water pressures with ground displacements. However, the solution neglects any variation of the coefficient of permeability with changes in effective stress. More precisely the analysis assumes that the ratio S_s/K is constant in time and space. A similar approximation is implicit in the conventional solution for consolidation of soft clays, which is a similar diffusion process involving release of pore water from saturated ground. The mechanism for pore water release in the later diffusion process is however different, due to differences in the relative compressibility of the skeleton and water, and to the magnitude of the water pressures. While during consolidation of clays, the mechanism for water release is compression of the soil skeleton; the transient flow into a deep tunnel excavated in a water-bearing rock formation is produced mainly by water expulsed from the voids due to expansion of pore water, as the pore water pressure is reduced.

5 ELASTIC ANALYSIS

Substituting the stress-strain relations for elastic behavior and the pressure gradient for radial flow into the equilibrium equation, and integrating the resulting differential equation, yields:

For $r \le R_w$:

$$\sigma_r^{'} = P_0^{'} - (P_0^{'} - P_i^{'})\frac{a^2}{r^2} - \frac{(P_{w0} - P_{wi})}{2(1-\nu)\ln\frac{R_w}{a}}\left[\frac{a^2}{r^2}\ln\frac{R_w}{a} + (\tfrac{1}{2} - \nu)(1 - \frac{a^2}{r^2}) - \ln\frac{R_w}{r}\right] \tag{8a}$$

$$\sigma_\theta^{'} = P_0^{'} + (P_0^{'} - P_i^{'})\frac{a^2}{r^2} + \frac{(P_{w0} - P_{wi})}{2(1-\nu)\ln\frac{R_w}{a}}\left[\frac{a^2}{r^2}\ln\frac{R_w}{a} + (\tfrac{1}{2} - \nu)(1 - \frac{a^2}{r^2}) + \ln\frac{R_w}{r}\right] \tag{8b}$$

$$u = \frac{(1+\nu)}{E}(P_0^{'} - P_i^{'})\frac{a^2}{r} + \frac{(P_{w0} - P_{wi})(1+\nu)r}{2E(1-\nu)\ln\frac{R_w}{a}}\left[\frac{a^2}{r^2}\ln\frac{R_w}{a} + (\tfrac{1}{2} - \nu)(1 - \frac{a^2}{r^2}) + (1-2\nu)\ln\frac{R_w}{r}\right] \tag{8c}$$

For $r = a$, Eq. (8c) reduces to:

$$u = \frac{(1+\nu).a}{E}\left[(P_0^{'} - P_i^{'}) + (P_{w0} - P_{wi})\right] \tag{9d}$$

For r ≥ R_w:

$$\sigma_r^{'} = P_0^{'} - (P_0^{'} - \sigma_{R_w}^{'})\frac{R_w^2}{r^2} \tag{9a}$$

$$\sigma_\theta^{'} = P_0^{'} + (P_0^{'} - \sigma_{R_w}^{'})\frac{R_w^2}{r^2} \tag{9b}$$

$$u = \frac{(1+\nu)}{E}(P_0^{'} - \sigma_{R_w}^{'})\frac{R_w^2}{r} \tag{9c}$$

The set of equations 8 show the detrimental effect of seepage forces on the stresses around the tunnel. Seepage forces reduce the effective radial stress, which is the minor principal stress, and increase the tangential stress, which is the major principal stress. Therefore, seepage forces increase the deviatoric stress σ_r-σ_θ, around the tunnel, while reducing the effective confining stress σ'_3.

On the other hand, Eq. 8c shows that even if the effective support pressure is equal to the far-field effective stress, there is still a ground displacement produced by seepage forces. According to Eq. (8d), the displacement at the wall face turns out to be the same as that computed for the total net pressure. However, the above result is true only for elastic conditions and only at the wall face.

6 ELASTO-PLASTIC ANALYSIS

The elastic solution is valid for effective support pressures greater than a critical pressure $P_i{}'_{crit}$ for which the effective stresses at the tunnel wall reach the failure criterion of the original ground. Using Eqs. (8) for $r=a$ and substituting into Eq. 1 yields

$$P_{i_{crit}}^{'} = \frac{2P_0^{'} - \sigma_c}{N_\phi + 1} + \frac{(P_{w0} - P_{wi})}{(1-\nu)(N_\phi + 1)} \tag{10}$$

For effective support pressures lower than the critical, the effective stresses induced in the ground following excavation will exceed the original ground strength, and a plastic zone of radius R_p will develop around the tunnel. The ground outside the boundary defined by R_p is assumed to remain elastic.

6.1 *Stresses and displacements in the elastic zone*

The elastic solution derived above is valid in the elastic zone. If the plastic zone is within the radius of influence of the tunnel (e.g. R_p<R_w) the solution is a set of equations similar to Eqs. (8), in which the tunnel radius *a,* is replaced by R_p, and the effective internal pressure P'_i, is replaced by the effective radial stress at the elastic/plastic interface, σ'_{rp}. On the other hand, if the plastic zone extends beyond R_w, the solution is a set of equations similar to Eqs. (9), in which the radial distance R_w is replaced by R_p and the effective stress σ'_{rw} is replaced by $\sigma'_{rp.}$

6.2 *Stresses in the plastic zone*

Substituting the failure criterion for the material in the plastic zone, into the equilibrium equation, and integrating the resulting differential equation, yields the following stress distribution in the plastic zone.

$$\sigma_r^{'} = \left[P_i^{'} + \frac{\sigma_{c_r}^*}{N_{\phi_r} - 1}\right]\left(\frac{r}{a}\right)^{N_{\phi_r}-1} - \frac{\sigma_{c_r}^*}{N_{\phi_r} - 1} \tag{11a}$$

$$\sigma_\theta^{'} = \sigma_{c\,r} + \sigma_r^{'}.N_{\phi\,r} \qquad \text{where} \quad \sigma_{c_r}^* = \sigma_{c_r} - \frac{(P_{w0} - P_{wi})}{\ln\frac{R_w}{a}} \tag{11b}$$

Equation (11b) shows that the effect of the seepage forces can be visualized as that of reducing the compressive strength of the ground in the plastic zone.

6.3 *Radius of plastic zone*

Considering equilibrium of effective radial stresses at the plastic/elastic boundary yields

$$\left(\frac{R_p}{a}\right)^{N_{\phi_r}-1} = \frac{\frac{2P_0' - \sigma_c}{N_\phi + 1} + \frac{\sigma_{cr}^*}{N_{\phi_r} - 1} + \frac{(P_{w0} - P_{wi})\ln\frac{R_w}{R_p}}{(N_\phi + 1)(1-\nu)\ln\frac{R_w}{a}}}{P_i' + \frac{\sigma_{cr}^*}{N_{\phi_r} - 1}} \tag{12}$$

The radius of the plastic zone is determined by solving iteratively Eq. (12). Equation (12) presumes that the plastic zone is within the radius of influence of the tunnel (e.g. $R_p<R_w$). If the plastic zone extends beyond de radius of influence, additional computations are required to determine the actual extent of the plastic zone. First Eq. (8a) is used to compute σ'_{Rw}, the effective radial stress at a R_w. Next a simplified version of Eq. (12) is used to compute the radius of the plastic zone, in which the effective support pressure P'_i is replaced by σ'_{Rw} and the water pressure gradient term is ignored. Such equation can be solved directly without any iterative procedure.

6.4 *Flowing ground condition*

Equation (12) will not converge (i.e. continuity of effective radial stresses at the plastic/elastic boundary cannot be accomplished) if the water pressure gradient, effective support pressure, and strength of the ground in the plastic zone are such that

$$\frac{(P_{w0} - P_{wi})}{\ln\frac{R_w}{a}} \geq P_i'(N_{\phi_r} - 1) + \sigma_{c_r} \tag{13}$$

For the above condition, which makes the denominator of Eq. (12) negative, the ground cannot resist the seepage forces and collapses into the tunnel. A 'flowing ground' condition will develop at the tunnel face, with the ground invading the tunnel.

Equation (13) includes three terms, which means there are three ways to handle flowing ground conditions. (a) Reduce the net water pressure with drainage (or compressed air), increase effective support pressure by adopting a stiffer support, and (c) increase ground strength with grouting.

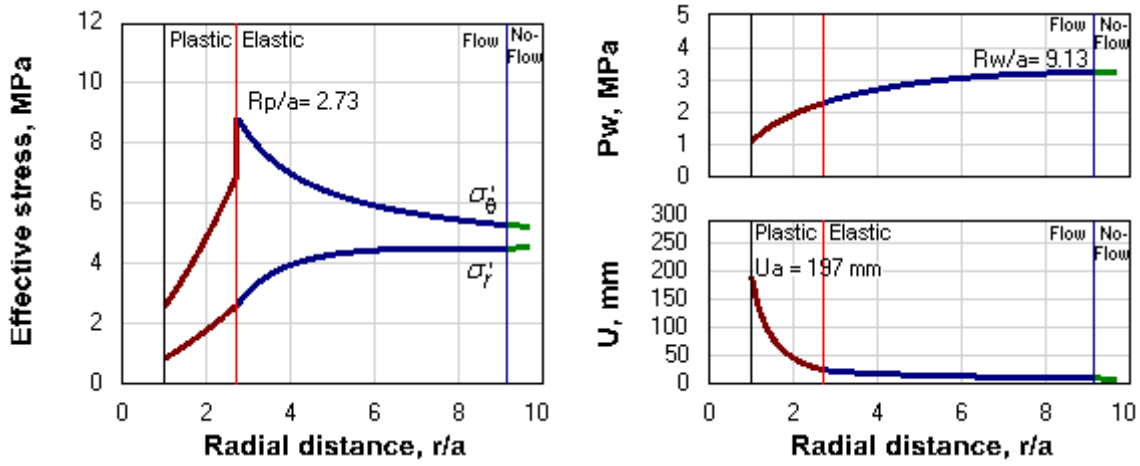

Figure 3. Effective stresses, water pressures and displacements around a tunnel.

6.5 *Displacements in the plastic zone*

Substituting the assumed flow rule into the strain compatibility equation, and integrating the resulting differential equation yields the following distribution of displacement within the plastic zone

$$u = \left[\frac{R_p}{r}\right]^{N_\alpha} \frac{(1+\nu)R_p}{E}\left[(P_0^{'} - \sigma_{R_p}^{'}) + (P_{w0} - P_{wp})\right] \tag{14}$$

where σ'_{Rp} and P_{wp} are the effective radial stress and pore water pressures at the plastic/elastic interface. The above solution allows computing the stress and displacement fields around the tunnel. Fig. 3 shows de distribution of pore water pressures, effective stresses and displacements for an application example described in section 9. The effective and water pressures at the wall face are Pi' = 0.84 MPa and P_{wi}= 1.09 MPa respectively, while the in situ effective stress and pore pressures are P'_0 = 4.9 MPa and P_{w0} = 3.2 MPa respectively.

7 TRANSIENT ANALYSIS

7.1 *Transient radius of influence*

The radius of influence R_w, has been treated so far as a constant distance beyond which the pore water pressure becomes equal to the original water pressure. However, in reality, such radius is transient in nature. Its initial value is the radius of the opening when the excavation is made, and it expands radially as time proceeds, until a maximum value is reached, corresponding to the development of a steady state condition.

Jacob and Lohman (1952) derived the first transient solution of the diffusion equation, for a tunnel subjected to a sudden, constant hydraulic head. The solution is a complicated one, which involves first and second kind zero-order Bessel functions. Recently, Perrochet (2005) developed a much simpler analytical solution, which yields essentially the same results. From the formula for the transient discharge in such solution, and accounting for the presence of a liner, the following equation for the transient radius of influence is obtained

$$\frac{R_w}{a} = 1 + \left[\frac{\pi K (P_{w0} - P_{wi})}{S_s a^2 P_{w0}} t\right]^{0.5} \leq \frac{R_{w_{\max}}}{a} \tag{15}$$

where t is the time elapsed since flow started at the section analyzed, and R_{wmax} is the maximum radius of influence corresponding to the final steady state condition.

7.2 *Progressive excavation*

Combining the above elasto-plastic solution and the concept of transient radius of influence, it is possible to evaluate the variation in time of the tunnel support requirements, extent of the plastic zone, distributions of pore water pressures, effective stresses, and displacements, during tunnel excavation, in terms of the tunnel advance rate. The analysis follows the approach used by Perrochet (2005) to determine transient discharge into a tunnel during progressive drilling.

Consider the progressive driving of a tunnel into a permeable zone at an average advance rate v, as illustrated in Figure 4. At time t, the tunnel face is located at a distance vt, and the time at which a position $x < vt$ was reached is x/v. Thus, the time elapsed since that position was reached and during which inflow occurred at that section is $t-x/v$, which is the time that goes into equation 15. Therefore, the transient radius of influence is a non-uniform function of space over the distance vt. Thus for a long tunnel, it is possible that by the time the tunnel face is near the end of the water-bearing zone ($x=L$), while the transient expansion of the radius of influence is beginning at such location, near the entrance to the water-bearing zone ($x=0$) the radius of influence may be approaching the steady state maximum.

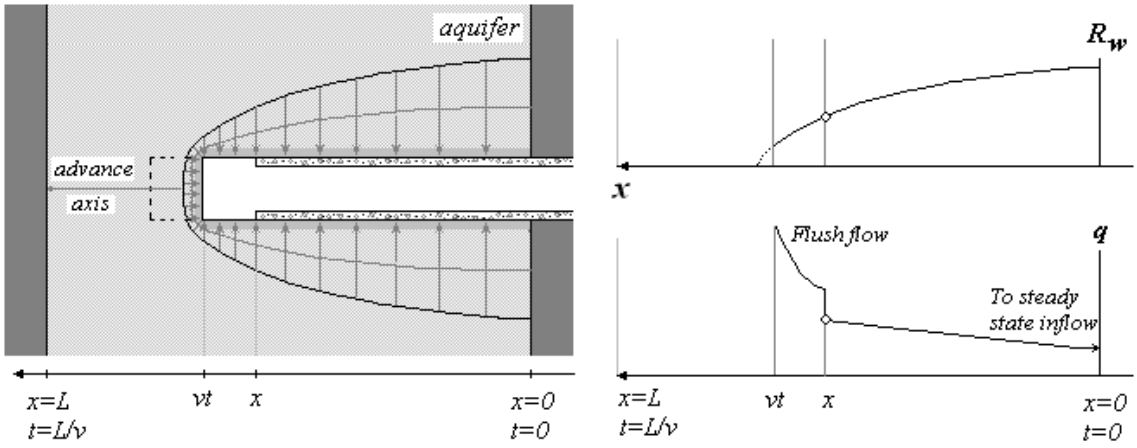

Figure 4. Flow regime, radius of influence *Rw*, and water inflow per unit length of tunnel, for a tunnel excavated at a constant velocity.

As a result, the radius of influence at the tunnel face, at the point where the support is being installed, and elsewhere, depend on the tunneling rate. If the tunnel is driven fast, the radius of influence along the tunnel will be small, resulting in large hydraulic gradients and seepage forces, which could cause stability problems at the face. For a slower advance rate, a larger hydraulic influence zone develops, reducing hydraulic gradients and seepage forces. Therefore, in poor permeable ground a slow rate of advance is preferred. However, on less pervious soft ground, with a short-term strength (undrained) greater than the long-term strength (drained), rapid advance improves stability. Analysis for the later case is not considered in this study. In both cases tunnel support, should be installed as fast as possible to provide early mechanical support.

On the other hand, as shown in Fig. 4, the larger initial heading inflow or "flush flow" (Heuer, 1995, Fernandez et al 2006), and the continuous decrease with time of the inflows per unit length that have been measured at tunnel walls as the steady state condition is approached, are all consistent with the concept of transient radius of influence. As the radius of influence expands the hydraulic gradient decreases and the inflow reduces as well.

7.3 *Steady state radius of influence*

Pore pressures, seepage forces, groundwater inflow, and the risk for instabilities are in general greatest immediately after excavation. The long-term condition would not be critical unless there is a significant deterioration of ground properties over time (e.g. due to weathering, slaking, creep, etc). Still, the long-term condition may be significant for the tunnel operation in terms of inflow. For long times, as the radius of influence expands away from the tunnel wall, the flow deviates from a circular fashion as the steady state condition is approached, and adjust to the site groundwater boundary conditions. Some possible steady state equilibrium configurations are shown in Figure 5.

The final steady state configuration of the water table depends on the available recharge. In case (a) recharge is from above and there is an unlimited amount of water available for recharge. The tunnel does not modify the horizontal water table. This is a case of confined flow where the ground remains saturated. In case (b) the water table is below the ground surface and the ground receives limited recharge water directly from the surface, mainly from precipitation. The recharge however is insufficient to maintain a horizontal water table and a significant drawdown develops. This is a case of unconfined flow where drainage of pore water makes part of the ground partially saturated. In case (c) the recharge is also limited, but greater than that in case (b), resulting in a small drawdown. In case (d) recharge is from an aquifer underlying the ground around the tunnel. Recharge is unlimited and the type of flow is confined.

Based on the flow net, one could estimate a steady state radius of influence R_{wmax} as a distance beyond which the pore pressure is not affected significantly by the presence of the tunnel. Typically R_{wmax} can be estimated as a factor (1 to 2) of the original groundwater pressure head P_{wo}/γ_w. Alternatively, an equivalent R_{wmax} could be computed as the radius of influence for a symmetrical flow regime that yields the same inflow as that of the actual flow net.

For case (a) in Fig. 5, the equivalent steady state radius of influence can be computed in terms of the depth to the tunnel D, using the actual analytical solution for flow rate (Harr, 1962), as

$$R_{w_{\max}} = 2D \tag{16}$$

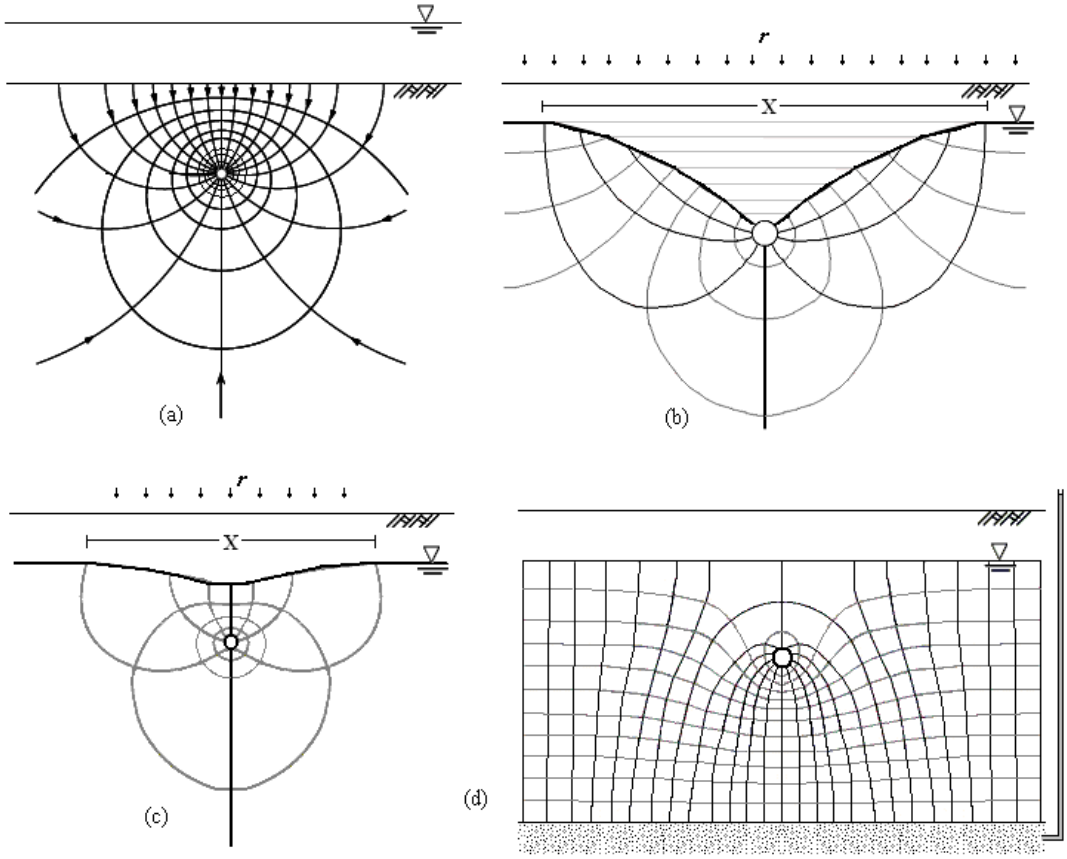

Figure 5. Steady state flow regime.

7.4 *Unconfined flow*

In cases of unconfined flow, such as in cases (b) and (c) in Figure 5, there are actually two different transient processes: expansion of the radius of influence and drawdown of the water table. Although both transient processes involve release of stored water, the mechanism of water release is different. During expansion of the radius of influence, water is released from saturated ground that remains saturated. The mechanism for water release is expulsion of pore water due mainly to expansion of pore water, as pore water pressure is reduced, and to a less extent, to compression of the ground skeleton. During the drawdown of the water table, water from storage is released by the mechanism of actually draining the pores of the ground, which makes part of the ground partially saturated (the depression cone).

Furthermore, the rate of the two transient processes is different. The rate of expansion of the radius of influence is controlled by the specific storage S_s, among other factors. On the other hand, the rate of drawdown is controlled by the storativity S (storage coefficient). The storativity is the percentage (by volume) of water that the ground could yield. For coarse-grained ground, the storage coefficient is equal to the porosity. For fine-grained ground the storage coefficient is smaller than the porosity because molecular and subsurface tension forces in the pore spaces keep some of the water in the voids.

The final width X_{max}, of the depression cone, for the steady state condition, can be determined based on the recharge r (e.g. mm/day) and the tunnel inflow as: $X_{max}=q/r$. A solution for the transient radius of the depression cone of an unconfined well from which water is pumped was derived by Chi (1994) as

$$X_t = X_{\max}\left[1 - e^{\frac{-4K(P_{w0}-P_{wi})_t}{S\gamma_w X_{\max}^2}}\right]^{0.5} \quad (17)$$

Thus, according to Eq. (17) the width of the drawdown cone expands exponentially with time, at a decreasing rate. Although Eq. (17) is applicable to a well or a vertical shaft instead of a horizontal tunnel, it suggests that the rate of drawdown is much slower than the rate of expansion of the radius of influence. Therefore, it appears that for unconfined flow cases, the expansion of the radius of influence predominates, in the early stages of flow after tunnel excavation, whereas drawdown dominates in the late stages.

8 HYDROMECHANICAL GROUND-SUPPORT INTERACTION

A ground-interaction analysis is used to determine the pressures acting on the lining, including the hydraulic pore water pressure P_{wi} and the mechanical effective pressure P'_i. The analysis is carried out for a time t, at which the tunnel support is installed. The support system considered includes a concrete lining and (or) rockbolts.

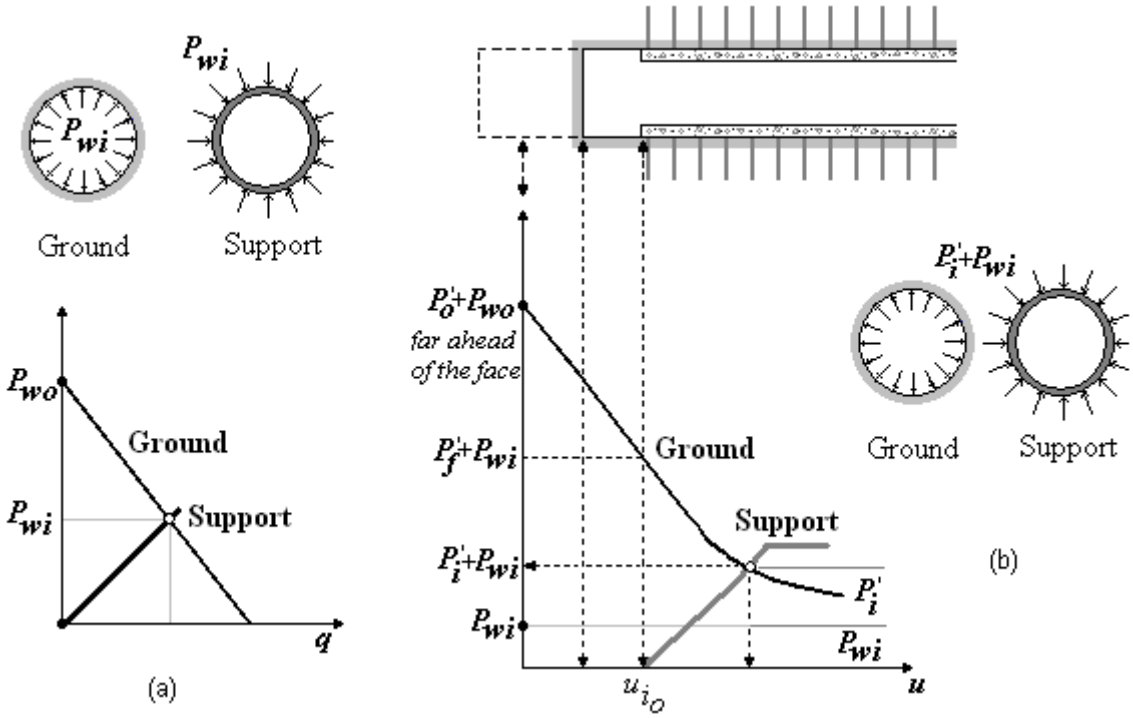

Figure 6. (a) Hydraulic ground-support interaction (b) mechanic ground-support interaction

The concrete or shotcrete lining is assumed to be porous and elastic-perfectly plastic. The properties of the lining are thickness t_c, Young's modulus E_c, Poisson's ratio ν_c, compressive strength f'_c, and coefficient of permeability K_c. The maximum support pressure P_{cmax} is computed based on the specified compressive strength.

The ungrouted mechanically or chemically anchored bolts are characterized by a stiffness K_b and a maximum support pressure P_{bmax}. These properties are computed based on the spacing, length, individual capacity, and other characteristics of the individual elements (Hoeck & Brown, 1980).

8.1 *Hydraulic interaction*

The flow rate seeping through the ground is

$$q_{ground} = \frac{2\pi K(P_{w0} - P_{wi})}{\gamma_w \ln \frac{R_w}{a}} \tag{18}$$

Whereas the flow rate through the lining is

$$q_{lining} = \frac{2\pi K_c P_{wi}}{\gamma_w \ln \frac{a}{a - tc}} \tag{19}$$

Figure (6a) illustrates the variation with P_{wi} of both, the flow rate through the lining and the seepage through the ground. Both are linear relations. From continuity, both flow rate quantities must be equal. Thus, as shown in Figure 6a, the inflow into the tunnel and the actual water pressure acting on the lining are represented by the intersection of the above two lines. If a relatively impervious lining is selected, the resulting water pressure acting on the lining is high, close to original water pressure P_{w0} and the tunnel inflow is minimal On the contrary, if a permeable lining is selected, the water pressure on the lining is minimal but the tunnel inflow is large.

8.2 *Hydromechanical interaction*

8.2.1 *Ground response curve*

Figure 6 illustrates the ground response curve as computed with the solution developed in the preceding section, by computing the wall displacement for the pore water pressure P_{wi} determined above, and for a variable effective support pressure P'_i. The effective support provided by the 'face effect' is shown in Fig. 6 as P'_f.

8.2.2 *Support characteristic curve*

The support characteristic curve is obtained by subjecting the lining to the hydraulic pressure P_{wi} and to a variable mechanical pressure P'_i. The characteristic curve is positioned at an initial displacement u_{io} representing the displacement that has occurred in the ground prior to the installation of the support. Such displacement can be estimated from a longitudinal deformation profile, as usual in the Convergence Confinement Method.

The solution for a porous liner subjected to hydraulic load P_{wi} and a mechanical load P'_i is obtained using the same approach followed to obtain the elastic solution in section 5.

The characteristic curve is:

$$u_a = \frac{P_i' a}{K'} + \frac{P_{wi} a}{K_w} + u_{i_0} \tag{20}$$

where

$$\frac{1}{K'} = \frac{(1+\nu_c)\left[(1-2\nu_c)a^2 + (a-t_c)^2\right]}{E_c\left[a^2 - (a-t_c)^2\right]} \text{ and } \frac{1}{K_w} = \frac{(1+\nu_c)}{2E_c(1-\nu_c)}\left[\frac{(1-2\nu_c)a^2 + (a-t_c)^2}{a^2 - (a-t_c)^2} + \frac{(1-2\nu_c)(1-\nu-\ln\frac{a}{a-t_c})}{\ln\frac{a}{a-t_c}}\right] \tag{21}$$

The tangential stress at the inner wall of the lining is

$$\sigma_\theta' = \frac{2P_i'}{1 - \frac{(a-tc)^2}{a^2}} + \frac{P_{wi}}{2(1-\nu_c)}\left[\frac{2}{1 - \frac{(a-tc)^2}{a^2}} + \frac{1-2\nu_c}{\ln\frac{a}{a-t_c}}\right] \tag{22}$$

The maximum support pressure generated by the concrete lining is the one that makes the tangential stress equal to the compressive strength of the material (i.e. $\sigma_\theta' = f_c'$).

Although the analysis assumes both support systems are installed at time *t*, in combining their characteristic curves, the actual sequence must be considered. As Fig. 7 illustrates, the sequence determines whether or not rockbolts help to support the external water pressure acting on the concrete lining. If shotcreting is done first followed by rock-bolting, rockbolts help to support

the fluid pressure. On the contrary, if the tunnel wall is bolted before shotcreting, the concrete liner alone has to support the fluid pressure.

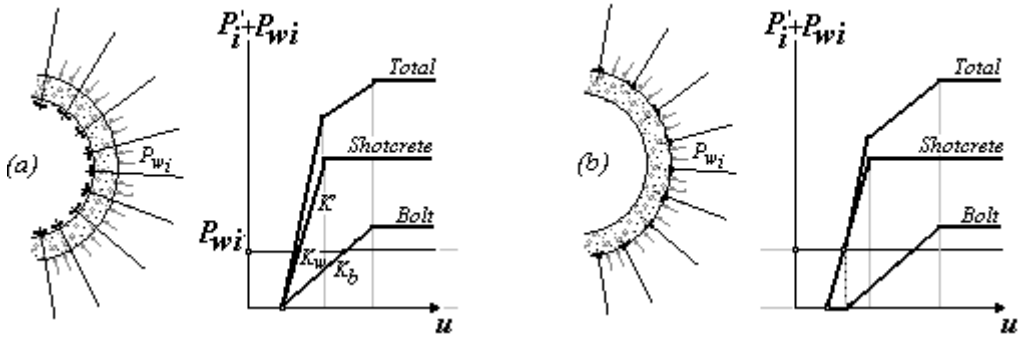

Figure 7. Combined support characteristic curve for two sequences of support installation. (a) shotcreting-bolting, (b) bolting-shotcreting

9 EXAMPLE

A 6 m diameter tunnel is excavated in a jointed sandstone at a depth of 300 m below the surface where the total in situ stress is P_o=8.1 MPa and the pore water pressure is P_{wo}= 3.2 MPa (pressure head 20 m above ground surface, Case (a) Fig. 5). The following material data is given:

- *Original rock mass*: E = 1.5 GPa, ν = 0.33, σ_c = 1 MPa, ϕ = 30º, K = 0.001 mm/sec, S_s = 0.00005 m^{-1}.
- *Rock mass in plastic zone*: σ_{cr} = 0.5 MPa, ϕ_r = 25º, α_r = 20º.
- *Shotcrete lining*: t_c = 200 mm, E_c = 16 GPa, ν_c = 0.25, f'_c = 50 MPa, K_c = 3x10^{-5} mm/sec.
- *Rockbolts*: 25 mm rockbolt, spacing pattern: 1.00 m x 1.00 m.

The support is installed at a distance of 2 m from the advancing tunnel face, about 4 hours after tunnel face advance. Based on the above distance and a longitudinal deformation profile, the initial ground displacement prior to the installation of the support is estimated to be 0.477 the maximum displacement away from face (displacement at which an unstable 'flowing ground' condition develops). The equivalent steady state radius of influence is R_{wmax}= 2 x 300 = 600 m.

This example was solved for: (1) the original parameters, (2) a liner with numerous shrinkage cracks and gaps represented by increasing its permeability an order of magnitude (K_c = 3x10^{-4} mm/sec), (3) no pore water pressure or conventional solution in terms of total stresses without considering pore water pressures and seepage forces. The results of the analysis are presented in Fig. 8 and summarized in Tables 1 and 2. Partial results for a case intermediate between 1 and 2 (K_c = 6x10^{-5} mm/sec) were presented in Fig. 3.

Comparing to case 3 (no pore pressures/ conventional analysis), case 1 demonstrates the effect of pore pressures and case 2 demonstrates the effect of seepage forces. In case 1, the liner is relatively impermeable as compared to the ground, thus seepage is limited. As Fig. 8a shows, the external water pressure in the liner is relatively high in this case. Hence the pore pressures in the ground near the tunnel remain high.

On the other hand, in case 2, the cracked lining allows more inflow and the release of the external pressure. As Fig 8a shows, the external water pressure in the lining is relatively low. Thus, there is a more significant hydraulic gradient in the ground in this case, leading to larger seepage forces. Fig. 8b shows the distribution of pore water pressure in the ground. The radius of influence is larger in the case of the cracked liner because the net hydraulic head is larger leading to a faster rate of expansion of R_w. Table 2 shows the expansion with time of R_w. Thus, even in permeable ground, it takes a few months to develop a steady state condition.

The ground reaction curves are shown in Fig 8c. The water pressure for each case is shown as a dotted line. The point of equilibrium is reached for much larger displacements in case 3, due to pore pressures and seepage forces, next in case 2, due to pore pressures and least in case 3, which includes neither pore pressures nor seepage forces.

Effective stresses and the extent of the plastic zone are shown in Fig. 8d. The conventional analysis gives the most optimistic results. The radius of the plastic zone increases from 2.12 to 2.64 because of the water pressures, and to 2.86 due to seepage forces.

Finally, the radial displacements are shown on Figure 8e. Pore pressures increase the radial displacement at the tunnel wall from 114 mm to 164 mm, and seepage forces to 243 mm.

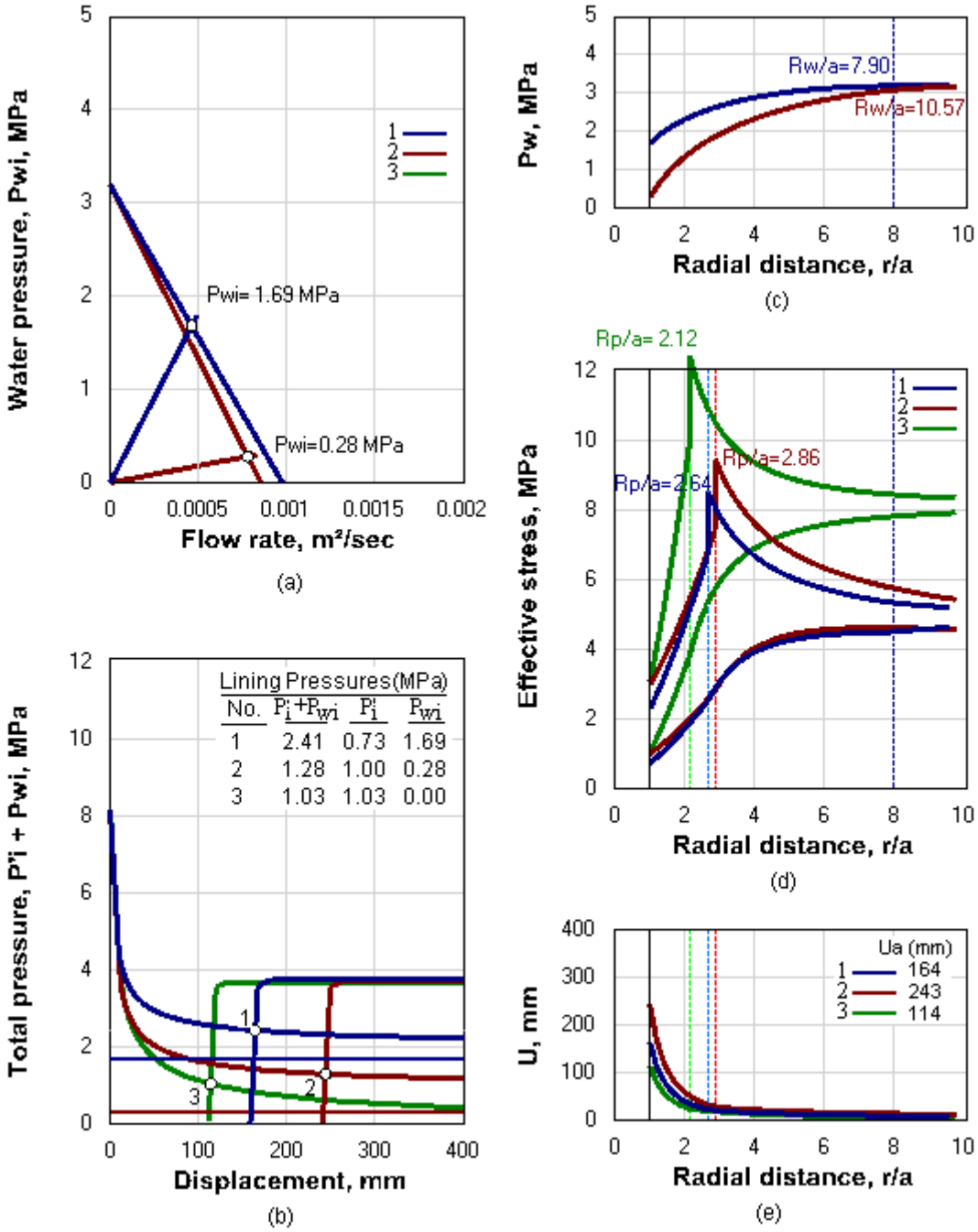

Figure 8. Hydromechanical interaction, and effective stresses, pore pressures, and displacement around tunnel for (1) original parameters (2) cracked liner (3) conventional analysis with no seepage forces

Table 1. Summary of Results.

No	P'_0 MPa	P_{w0} MPa	P'_i MPa	P_{wi} MPa	U_a mm	Rp/a -	Rw/a -
1	4.9	3.2	0.73	1.69	164	2.64	7.90
2	4.9	3.2	1.00	0.28	243	2.86	10.57
3	8.1	0	1.03	0.00	114	2.12	-

Table 2. Expansion of Radius of Influence with Time.

Time	0	2hrs	4 hrs	12 hrs	1 day	1 week	1 month	3 months	6 months
Case 1, R_w (m):	3	16.9	23.7	41.0	58.3	158	333	586	600
Case 2, R_w (m):	3	23.1	31.7	53.1	74.1	192	397	600	600

10 CONCLUSIONS

Seepage forces generated during tunnel excavation may cause serious instability problems, which cannot be assessed with current ground interaction analyses. An elasto-plastic solution has been derived that includes the effect of pore water pressures and seepage forces, on the stress and displacement field around the opening, and on the extent of the plastic zone. The conditions for development of 'flowing ground' at the tunnel face have been identified. The transient nature of the hydraulic radius of influenced has been described and a procedure to predict its transient expansion has been proposed. The effects of the progressive excavation have been discussed. Procedures for hydromechanic ground interaction analysis have been developed. An application example demonstrated the significant effect of pore water pressures and seepage forces on the behavior of tunnels. The solution is applicable to tunneling in weak rocks, highly fractured rocks, crushed rocks (e.g. fault zones), and general soil-like materials, subjected to high water pressures.

REFERENCES

Alvarez, T.A. 1997. A Study of the Coupled Hydromechanical Behavior of Jointed Rock Masses Around Pressure Tunnels, Ph.D. Thesis, University of Illinois at Urbana-Champaign, Urbana, IL.

Barbosa, R.E. 1990. Discrete Element Models for Granular Materials and Rock Masses, Ph.D. Thesis, University of Illinois at Urbana-Champaign, Urbana, IL.

Barbosa, R.E. 2009. EngSolutions TUNNEL, User's Manual. EngSolutions, Inc., Ft. Lauderdale, FL.

Brown, E.T., Bray, J.W., Ladanyi, B., Hoek, E. 1983. Ground response curves for rock tunnels. ASCE J. Geotech. Eng. Div. 109 (1), 15-30

Bobet, A. 2003. Effect of pore water pressure on tunnel support during static and seismic loading. Tunneling and Underground Space Technology 18, 377-393.

Chu, S.T. 1994. Transient Radius of Influence Model. ASCE J. Irrig. and Drainage Eng. 120 (5), 964-969

Fernandez, G. and J.S. Moon 2006. Evaluation and assessment of inflow rates in tunnels excavated in jointed rock mass. VI South American Rock Mechanics Congress, Cartagena, Colombia.

Harr, M.E. 1962. Groundwater and seepage. McGraw-Hill Book Co, Inc.., New York, N.Y.

Hendron A.J., and A.K. Aiyer 1972. Stresses and Strains Around a Cylindrical Tunnel in an Elasto-Plastic Material with Dilatancy. Omaha District, Corps of Engineers, Technical Report No. 10, Omaha, NE..

Heuer, R.E. 1995. Estimating rock tunnel water inflow. Rapid Excavation and Tunneling Conference, Chap. 3, pp. 41-60.

Jacob CE, Lohman S.W. 1952. Nonsteady flow to a well of constant drawdown in an extensive aquifer. Trans AGU 33(4):559-569

Li, X. 1999. Stress and displacement fields around a deep circular tunnel with partial sealing. Computers and Geotechnics 24, 125-140.

Lee, I. and Nam, S. 2001. The study of seepage forces acting on the tunnel lining and tunnel face in shallow tunnels. Tunneling and Underground Space Technology 16, 31-40.

Lee, I. and Nam, S. 2004. Effect of tunnel advance rate on seepage forces acting on the underwater tunnel faces. Tunneling and Underground Space Technology 19, 273-281.

Marulanda, A., C. Marulanda and R. Gutierrez 2008. Experiences in tunnel excavation by the conventional method and by TBMs in the Andes Mountain Range. Case histories. I South American Symposium on Rock Excavations, Bogota, Colombia.

Perrochet, P. 2005. A simple solution to tunnel or well discharge under constant drawdown. Hydrology Journal 13, 886-888.

Perrochet, P. 2005. Confined flow into a tunnel during progressive drilling: an analytical solution. Ground Water 43, No. 6, 943-946.

Shin, J.H., Potts D.M., and Zdravkovic L. 2005. The effect of pore-water pressure on NATM tunnel linings in decomposed granite soil. Canadian Geotechnical Journal 42, 1585-1599.

Singh, B. and R.K. Goel (2006) "Tunneling in Weak Rocks, Volume 5" Geo-Engineering Book Series, Elsevier.